Monte-Carlo based investigation of individual dosimetry in deep geological repository for high-level nuclear waste with consideration of realistic body postures

Bo Pang [a,b], Frank Becker [c,*], Volker Metz [c]

[a] Advanced Nuclear Energy Research Team, Department of Nuclear Science and Technology, College of Physics and Optoelectronic Engineering (CPOE), Shenzhen University (SZU), 518060 Shenzhen, China
[b] Institute of Nuclear Power Operation Safety Technology, affiliated to the National Energy R & D Center on Nuclear Power Operation and Life Management, 518060 Shenzhen, China
[c] Institute for Nuclear Waste Disposal (INE), Karlsruhe Institute of Technology (KIT), Hermann-von-Helmholtz-Platz 1, 76344 Eggenstein-Leopoldshafen, Germany

A B S T R A C T

Deep geological disposal with provisions for retrieval is one of the most promising strategies for the def inite management of high level nuclear waste. However, retrieval of disposed waste might require cer tain extensive work of personnel near the waste package that might also enhance the level of radiation exposure. Hence, a precise estimation of the personal dose with consideration of realistic body postures is highly desired for optimization of individual working scenarios. In this study, the near field of a generic geological disposal facility was modeled with a horizontal emplacement drift in saline host rock. Inside the drift, a shielded disposal cask loaded with spent nuclear fuel was placed on the ground. A whole body stylized phantom with moveable limbs was applied to represent a reference worker. Several relevant realistic body postures that might be encountered in a disposal facility were investi gated. The corresponding radiation exposure was calculated and compared with a general purpose Monte Carlo code.

Keywords:
High-level nuclear waste (HLW)
Deep geological disposal
Individual dosimetry
PIMAL phantom
Realistic body posture
Monte Carlo simulation

1. Introduction

Disposal in deep geological formations with provisions for retrieval has been considered as one of the most promising strate gies to deal with the complex challenge arising from long term and safe disposal of high level nuclear waste (HLW), especially of spent nuclear fuel (SNF) generated from commercial utilization of nuclear power in the past and upcoming decades. Currently, there is a strong interest in retrievability of the waste packages during the operational phase and initial period of the post operational of a geological disposal facility as response to uncertainties regarding the adequacy of the disposal arrangements and to avoid irre versible steps (NEA, 2010, 2012; Röhlig et al., 2017; USNWTRB, 2018). However, retrieval of more than a few waste packages at a late stage of emplacement or in the post operational phase would be a major decision with considerable implications to work ers (NEA, 2010, 2012). If decided upon at later stages of disposal, retrieval of the disposed nuclear waste might require handling of the retrieved waste packages and thereby certain amount of exten sive work performed by the workers nearby the nuclear waste packages, which is directly related to an enhanced level of radia tion exposure of the workers. Hence, a precise estimation of the individual personal dose with consideration of realistic body pos tures during individual working scenarios in the non uniform radi ation field around nuclear waste packages is highly desired, at least for optimizing working scenarios in the planning phase.

The effective dose, whose definition has been revised in its lat est recommendation (ICRP, 2007) was suggested by ICRP as a ref erence dose quantity to assess the occupational exposure for external irradiation. As a revision of the previous ICRP publication 74 (ICRP, 1997), the latest set of dose conversion coefficients has been also reported in the ICRP publication 116 (ICRP, 2010), in which organ absorbed dose and effective dose conversion coeffi cients were calculated for various standard irradiation geometries, including antero posterior (AP), postero anterior (PA), left and right lateral (LLAT, RLAT), rotational (ROT) and isotropic (ISO) as specified by ICRP (2007). The ICRP/ICRU reference adult female and male voxel phantom as defined in the ICRP publication 110 (ICRP, 2009) were used for these calculations and all the computa tional phantoms were assumed to be in the vertical upright posi tion. However, the irradiation situation of a worker inside a

* Corresponding author.
E-mail address: frank.becker@kit.edu (F. Becker).

disposal facility differs to that of a phantom in the vertical upright posture exposed in the standard irradiation geometries, mainly because of the following two aspects: first, the irradiation geome try in the radiation field of a disposal facility cannot be readily rep resented with standard irradiation geometries; and second, probably more important, worker's body postures during realistic working scenarios in the disposal facility cannot be represented with the vertical upright posture. As pointed out for instance by Dewji et al. (2017), the vertical upright phantom position could largely underestimate the absorbed dose of certain important organs in the phantom positions with half and full bent torso. Therefore, it is important that the influence of realistic body pos tures must be taken into account when conducting an accurate estimation of the radiation exposure in geological repository.

Fig. 1 summarizes the approach of this work to investigate the individual dosimetry in a generic deep geological disposal facility for HLW. Three steps are considered. The first two steps have already been conducted in previous studies of our group, for which the most important conclusions derived are also included in the figure as well as in the subsequent description.

(a) Calculation of the radiation field in a generic geological disposal facility for high-level nuclear waste.
In our previous studies (Pang et al., 2016, 2017a), a horizon tal emplacement drift inside a rock salt formation was defined as a generic deep geological disposal facility, in which a nuclear waste package, simulated with a POLLUX® type shielded cask (Janberg and Spilker, 1998) loaded with spent nuclear fuel (SNF) was placed on the ground. Geomet rical details of the emplacement drift were adopted from a generic concept proposed for disposal in rock salt (Stahlmann et al., 2015).
Radiation source for the external irradiation on workers was then defined by SNF inventory contained in the POLLUX® type cask. Since the radiological characteristics of SNF depend on a variety of factors, an individual analysis of each spent fuel assembly (FA) is neither feasible, nor necessary. Instead, a model FA was defined in such way, that the iso tope composition and burnup of the model FA represent that of the average inventory of used fuel elements discharged from pressurized water reactors (Peiffer et al., 2011). In this study, the HLW inventory in the POLLUX® type cask contains a model pressurized water reactor FA, which consists of two thirds UOX spent fuel and one third MOX spent fuel accord ing to the mixed loading strategies used in German nuclear power plants (Janberg and Spilker, 1998).
An average burnup of 55 GWd/tHM (gigawatt days per met ric ton of heavy metal) was assumed for both UOX and MOX spent fuel. To derive a relevant cooling time of the SNF after discharge from the reactor core, we consider both the dura tion of interim storage of used fuels in many countries, which might be far longer than fifty years (Herm et al., 2018; Spykman, 2018), and the duration of emplacement in the geological disposal facility. Since it must be ensured that the disposed waste package can be retrieved during the operating phase or the early post operation phase of the repository probably lasting in the order of 100 years, the age, i.e. the cooling time of the SNF counting from unloading of the FA from the reactor core, was adopted to be in average of 100 years, which corresponds to the time frame when a retrieval of the HLW waste package becomes most likely.

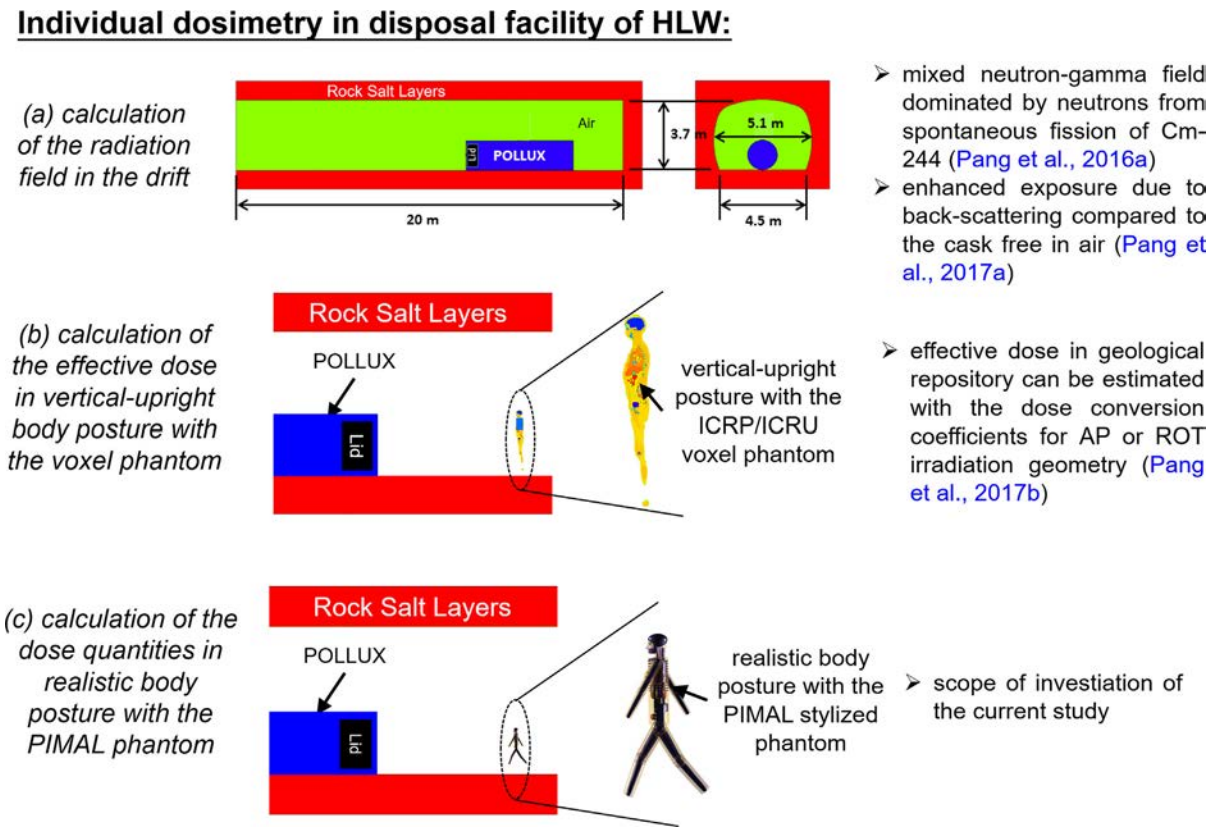

Fig. 1. Individual dosimetry in disposal facility of HLW: (a) calculation of the radiation field in the drift, (b) calculation of the effective dose in vertical-upright body posture with voxel phantom and (c) calculation of the effective dose in realistic body posture articulated with the PIMAL phantom.

It was found out that the 100 years old SNF would create a mixed gamma neutron radiation field inside the emplace ment drift. In the time frame of possible retrieval of the dis posal HLW, the personal exposure in the emplacement drift is dominated especially by those neutrons stemming from spontaneous fission of transuranic heavy isotopes (for instance Cm 244). Furthermore, the radiation field in the geological repository is characterized by back scattered radiation due to the surrounding host rock layers. Conse quently, the geometrical conditions of the occupational exposure in the disposal facility cannot be readily repre sented by the standard ICRP irradiation geometries.

(b) Calculation of the effective dose in vertical-upright body posture with the ICRP/ICRU voxel phantom in the emplacement drift.

Since geometrical conditions of the occupational exposure in the geological facility cannot be readily represented by the standard irradiation geometries defined by ICRP, it is of interest to calculate the reference level of the occupational radiation exposure in terms of effective dose. The issue to be clarified is whether a standard ICRP irradiation geometry, or a combination of several standard irradiation geometries could be suitable to approximate the irradiation situation in the deep geological disposal facility. If it is the case, the dose conversion coefficients for the standard irradiation geome tries can then be readily applied in deep geological disposal facilities to obtain the reference level of the occupational radiation exposure in terms of effective dose.

This investigation was conducted in the previous study (Pang et al., 2017b), in which the ICRP/ICRU reference adult voxel phantom (ICRP, 2009) was placed at various distance and different body orientations with respect to the lid sur face of a disposed POLLUX® type cask in the emplacement drift. It was found that depending on the orientation of the worker in the drift, the dose conversion coefficients for the AP or the ROT geometry given in the ICRP publication 116 (ICRP, 2010) could be used for an adequate estimation of the effective dose in the rock salt drift. For the case of the front body side facing the POLLUX® lid surface, dose conver sion coefficients for the AP geometry can provide an ade quate estimation of the effective dose in the drift. For other orientations of the worker, i.e. when the rear body side or the lateral body side facing the POLLUX® lid surface, the dose conversion coefficients for the ROT geometry should be used. However, these calculations were performed with the voxel phantom in the vertical upright position, the influ ence of realistic body postures are considered subsequently.

(c) Calculation of the dose quantities in realistic body postures in the emplacement drift.

Although the ICRP/ICRU reference voxel phantoms have great anatomical details, the phantoms are in the vertical upright posture. More importantly, generating different pos tures using only voxel geometry is problematic and the required computational effort is quite high. Therefore, a whole body stylized phantom with movable limbs, i.e. the Phantom with Moving Arms and Legs (PIMAL) (Akkurt et al., 2007) was applied to represent a reference worker inside the drift. With the PIMAL phantom, realistic body pos tures can be represented, which enables a more realistic estimation of the individual radiation exposure during working scenarios.

Step (c) as described above is the scope of the current study. Since neutron dose dominates the personal exposure in the radia tion field of the emplacement drift, it is of highly interest to inves tigate the neutron induced exposure when considering the influence of realistic body postures. The present study focuses on investigating how organ absorbed dose and effective dose vary, when realistic occupational postures differing to the vertical upright were taken into account. For consistency with the previous studies of the step (a) and (b), the generic geological disposal facil ity was modeled with a horizontal emplacement drift covered by rock salt layers as host rock formations. Inside the drift, a nuclear waste package, simulated with a POLLUX® type cask loaded with 10 model spent model FAs was placed on the ground. Radiation exposure assessment for realistic body postures in the emplace ment drift, including those representing a sitting person, a walking person and a person with full bent torso, was calculated with the general purpose Monte Carlo code MCNP6 (Pelowicz, 2013). The standard vertical upright body posture was used as reference for comparison with the realistic body postures.

2. Methods and methodology

Based on the above introduction, a comprehensive investigation regarding individual dosimetry in geological disposal facility asso ciated with the PIMAL phantom accounting for the influence of realistic body postures was defined. The complete study was decomposed into two parts with detailed description given as follows:

(I) Calculation of neutron organ and effective dose conversion coefficients in standard irradiation geometries with the PIMAL stylized phantom in vertical-upright body posture.

In this part of study, the PIMAL phantom in vacuum was irradiated with the standard irradiation geometries defined by ICRP, including AP, PA, LLAT, RLAT and ISO. In all the stan dard irradiation geometries, the PIMAL phantom was in the vertical upright position. The latest set of dose conversion coefficients provided by ICRP (ICRP, 2010) was used as refer ence. Dose conversion coefficients obtained with the PIMAL phantom in vacuum were compared with them, in order to quantify the difference between the PIMAL phantom and the ICRP/ICRU reference voxel phantom. This part of study is devoted to assess the PIMAL phantom for calculating neu tron dose quantities in the energy range of interest.

(II) Calculation of the radiation dose in deep geological disposal facility of HLW with realistic body postures represented by the PIMAL phantom.

The PIMAL phantom was now placed at a certain distance relative to the lid surface of the POLLUX® type cask disposed in the emplacement drift. For the vertical upright posture and the investigated realistic postures representing a sitting person, a walking person and a person with full bent torso, especially those organs/tissues which are sensitive to exter nal radiation exposure (i.e. organs with relative higher tissue weighting factors w_T and hence larger contribution to the effective dose) were carefully assessed. Finally, a com parison of the radiation dose with respect to the different body postures could be conducted.

The default body posture of the PIMAL is in the vertical upright position, while a user graphic interface was employed in the PIMAL software to adjust different realistic postures and to generate cor responding input files for radiation transport simulations for the dose calculations with MCNP6. The mode "n, p" was used as default. Hence, the thick target bremsstrahlung model (TTB) was employed. The MCNP F6 tallies were preset by PIMAL to estimate the absorbed dose of the organs. The default library in MCNP6, i.e. the ENDF/B VII.1 nuclear and atomic data, was employed. The

variance reduction technique "geometry splitting" with individu ally assigned particle importance was used. This technique sug gested for deep penetration problems is adopted in this study, as in particular the simulation of radiation transport and interaction inside the heavy shielded POLLUX® cask requires such an approach. Detailed description regarding the modeling of POLLUX cask in MCNP6 has been published in previous papers (Pang et al., 2016; Pang and Becker, 2017). For convenience, only the most important points were mentioned here. The POLLUX cask was split into several thin sub layers with individually assigned particle importance, so that a layer farther away from the neutron source was assigned to have a greater importance than a layer clo ser to the neutron source. Using the example of the PIMAL phan tom inside the emplacement drift, the waste inventory (radiation source) was assigned a particle importance of unity. The further out the particles move in the cask, the more the importance was gradually increased up to 20.

2.1. Part I: Calculation of neutron organ and effective dose conversion coefficients in standard irradiation geometries with PIMAL stylized phantom in vertical upright body posture

Concerning the HLW inventory investigated in the current study, i.e. the 100 years old SNF, the majority of the source neu trons have energies ranging between 0.1 MeV and 10 MeV. In order to obtain the fluence to dose conversion coefficients in this energy range, simulations with ICRP standard irradiation geometries (in cluding AP, PA, LLAT, RLAT and ISO) were performed with mono energetic neutrons in the range of thermal neutron energy (2.5×10^{-8} MeV) up to 20 MeV. The investigated dose quantities include organ absorbed doses and effective dose. In terms of effec tive dose calculation, the most recent methodology defined in (ICRP, 2007) was applied, in which the computation of equivalent doses in organs and tissues of both female and male phantom is required, in order to drive the gender averaged quantity of effec tive dose[1].

As an example, Fig. 2 shows the PIMAL female phantom in vertical upright posture for PA irradiation geometry. The base point (0, 0, 0), as indicated with the (blue) cross sign in the figure was located at the center of the pelvic area of the PIMAL phantom. Organ/tissue absorbed dose due to the incident source neutrons was calculated with the kerma approximation, i.e. with the F6 tally in MCNP6, which calculates the energy deposition due to the inci dent neutrons in the respective organs/tissues. However, it must be pointed out, that secondary gamma rays stemming from neutron interaction with tissue materials, especially the 2.2 MeV gamma ray due to neutron capture by hydrogen, play also an important role. Consequently, both the energy deposition due to neutrons and photons should be included in the F6 tally, i.e. "F6:n,p". The most important setting in the MCNP6 simulations are summarized as follows:

- Standard irradiation geometries investigated including: AP, PA, LLAT, RLAT and ISO;
- Both the PIMAL female and male phantom were defined in the vertical upright posture, immersed in a vacuum defined by a sphere centered at the base point (0, 0, 0) with a radius of 200 cm;
- For the AP, PA, LLAT and RLAT irradiation geometry, the neutron source was defined as a rectangular plane source with a dimen sion of 200 cm $\times$ 200 cm at a distance of 1 m to the PIMAL phantom base point (0, 0, 0). For the ISO irradiation geometry, however, the neutron source was defined directly on the spher ical surface centered at (0, 0, 0) with the radius of 200 cm. The dimension of the source plane and the source sphere was cho sen rather arbitrarily, so that the neutron source in all the irra diation geometries is large enough to cover the whole PIMAL phantom;
- The mono energetic neutron energies of the source amount to: 2.5×10^{-8} MeV, 0.0001 MeV, 0.001 MeV, 0.01 MeV, 0.1 MeV, 0.2 MeV, 0.5 MeV, 1 MeV, 2 MeV, 5 MeV, 10 MeV and 20 MeV;
- All the MCNP6 simulations were run for 1×10^9 particles, with statistical errors converging predominately within $< 0.5\%$ also for small or deep organs/tissues.

2.2. Part II: Calculation of the radiation dose in deep geological disposal facility of HLW with realistic body postures represented by the PIMAL phantom

As depicted in Fig. 3, three relevant realistic body postures rep resenting a sitting and a walking person, as well as a person with full bent torso, were investigated in this study.

In the figure only the PIMAL female phantom is shown, while the same posture definition was also adopted for the PIMAL male phantom. The vertical upright posture was used as reference for the other body postures. The PIMAL phantom was then placed in the emplacement drift at a certain distance to the lid surface of a POLLUX® type cask. As described previously, 10 spent model FAs with an age of 100 years represent the loading of the cask. The total neutron production rate of the SNF loaded in the POLLUX® type cask amounts to 1.054×10^9 n s^{-1}. The corresponding energy spec trum was already calculated in a previous study (Pang and Becker, 2017). Fig. 4 depicts the case of a PIMAL female phantom in sitting posture at 2 m distance to the lid surface of the POLLUX® type cask.

Details about the MCNP6 modeling of the emplacement drift and of the POLLUX® type cask can be found in the previous studies (Pang et al., 2016 and Pang and Becker, 2017), respectively. In this study, MCNP6 calculation of the organ absorbed dose with the F6 tally accounting for the energy deposition was conducted for both PIMAL female and male phantom, in sitting, walking and full bent postures, at distances of 1 m and 2 m, respectively. Furthermore, simulations were also performed for the PIMAL phantom in the vertical upright posture at the same distance, which served as ref erence for comparison with the other postures. The variance reduc tion technique "geometrical splitting" with individual importance assignment was conducted when modeling the POLLUX® type cask, so that the MCNP6 simulations for the distance of 1 m and 2 m were run for 1×10^8 and 2×10^8 particles, respectively, with sta tistical errors converging predominately within $< 2\%$ for large organs/tissues and within $< 5\%$ for small or deep organs/tissues.

3. Results and discussion

3.1. Organ absorbed dose conversion coefficient with the PIMAL phantom in vertical upright position

As an example, Fig. 5 compares for the PA irradiation geometry and incident neutron energy up to 20 MeV, the organ absorbed dose conversion coefficients (both female and male) obtained by the stylized PIMAL phantom with the corresponding coefficients provided by ICRP (ICRP, 2010) with the ICRP/ICRU voxel phantom. The ratio of the organ absorbed dose conversion coefficients obtained by the PIMAL stylized phantom in the current study to

[1] To be more precisely speaking, the very term of effective dose can only be used specifically with the ICRP/ICRU voxel phantom. Consequently, in this study a dose quantity according to the definition of effective dose but with the PIMAL phantom instead of the ICRP/ICRU voxel phantom was calculated similarly to the investigations in (Hiller and Dewji, 2017; Bales et al., 2018).

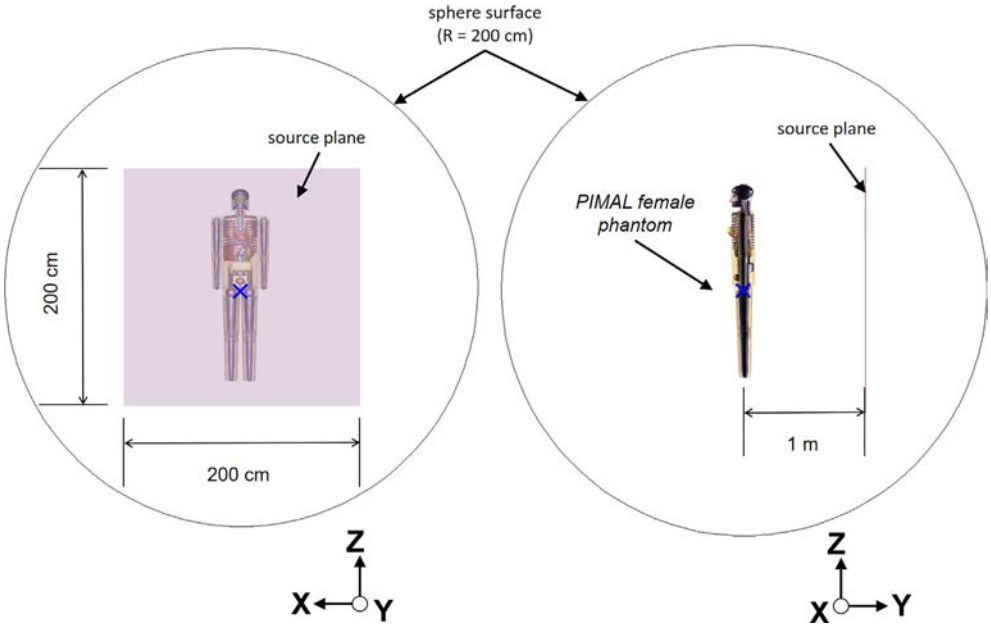

Fig. 2. PIMAL female phantom in vertical-upright posture for PA irradiation geometry. (For a better visibility of the source plane, the reader is kindly referred to the web version of this article.)

Fig. 3. PIMAL female phantom representing four realistic body postures. The vertical-upright posture was used as reference for comparison with a sitting, a walking and a full-bent person.

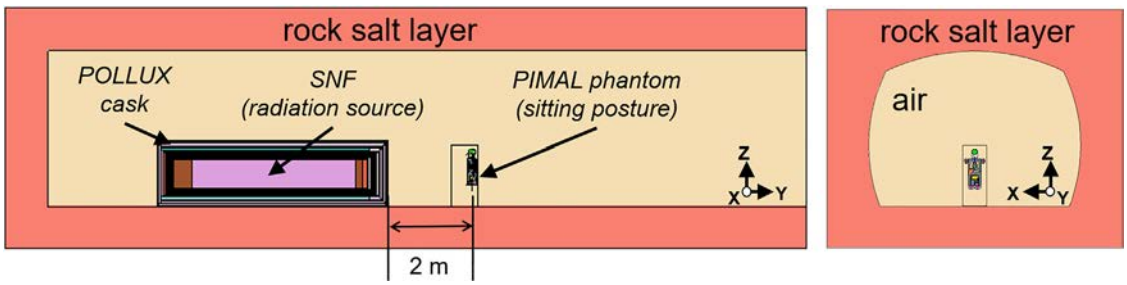

Fig. 4. PIMAL female phantom representing a sitting person in the emplacement drift at 2 m distance to the disposed POLLUX® type cask.

those given by ICRP, termed as "Ratio Stylized/Voxel", was plotted for all the organs used to define the effective dose. Overall, due to the relatively large difference in organ size, organ position, mate rial composition etc. between the PIMAL stylized phantom and its voxel counterpart, the organ absorbed dose obtained with the two phantoms agree with each other with a relative deviation within the interval of $\pm 50\%$.

However, for external irradiation, the most important quantity to be considered is the effective dose whose definition was recently revised in the ICRP recommendation 2007 (ICRP, 2007). Calculation of the effective dose requires a gender averaged organ equivalent dose, which is the average value of the female and male organ absorbed dose multiplied with the radiation weighting factor w_R in dependence of the neutron energy. However, the contribution

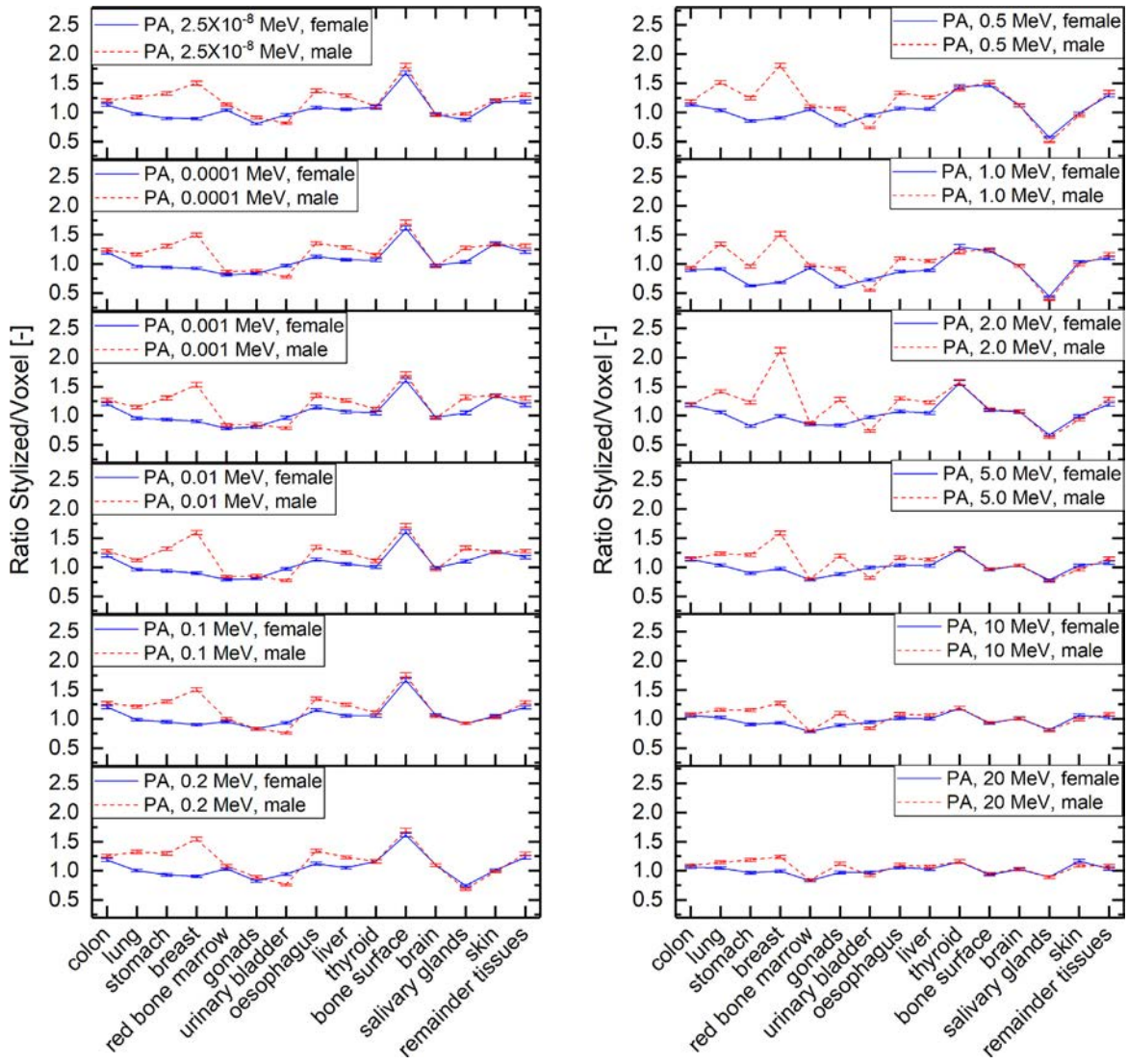

Fig. 5. Comparison of the absorbed dose coefficients obtained by PIMAL phantom in vertical-upright posture with those given in ICRP publication 116 (ICRP, 2010) for the PA irradiation geometry.

of different organs to the effective dose is also different, which is considered with the so called tissue weighting factor w_T. Fig. 6 compares then the relative organ contribution to the effective dose for the PA irradiation geometry and the incident neutron energies up to 20 MeV. The plot value "Relative Contribution" for a given organ was defined according to:

$$Relative\ Contribution \quad \frac{\left(D_{T,gender\ \ averaged} \times w_{R,incident\ \ source\ \ neutron}\right) \times w_T}{E} \tag{1}$$

where $D_{T,gender\ \ averaged}$ stands for the gender averaged organ absorbed dose. $w_{R,incident\ source\ neutron}$ and w_T are the energy dependent radiation weighting factor of the incident source neutron and the tissue weighting factor of the organ, respectively. E is then the effective dose. Despite of the relatively large difference observed for the gender specific organ absorbed dose, the relative contribution of the organs to the effective dose exhibits a quite similar behavior. In the neutron energy range of interest, no large difference was observed between the PIMAL stylized phantom and the voxel phantom. The same organs/tissues defined respectively in the PIMAL stylized phantom and in the ICRP/ICRU voxel phantom contribute also a similar share to the effective dose.

Finally, Fig. 7(a) (e) compare for the standard irradiation geometries AP, PA, LLAT, RLAT and ISO, the effective dose conversion coefficients obtained by the PIMAL phantom in vertical upright posture with the respective coefficients provided by ICRP obtained by the ICRP/ICRU reference voxel phantom as given in the publication 116 (ICRP, 2010). Also included in the subfigures for the AP, PA, LLAT and RLAT geometries are the dose conversion coefficients reported by Bales et al. (2018) with the same PIMAL phantom as in the current study. Noted that for the ISO irradiation geometry no data was available in the publication of Bales et al. (2018). Finally, Fig. 7(f) summarizes for the investigated irradiation geometries the ratio between the ICRP coefficient and the coefficients obtained with PIMAL phantom in the current study, which can also be found in the Table 1 in appendix of the current study.

It is observed:

- In general, the effective dose conversion coefficients obtained in the current study coincide with those reported by Bales et al. (2018) with the same PIMAL phantom. However, compared to

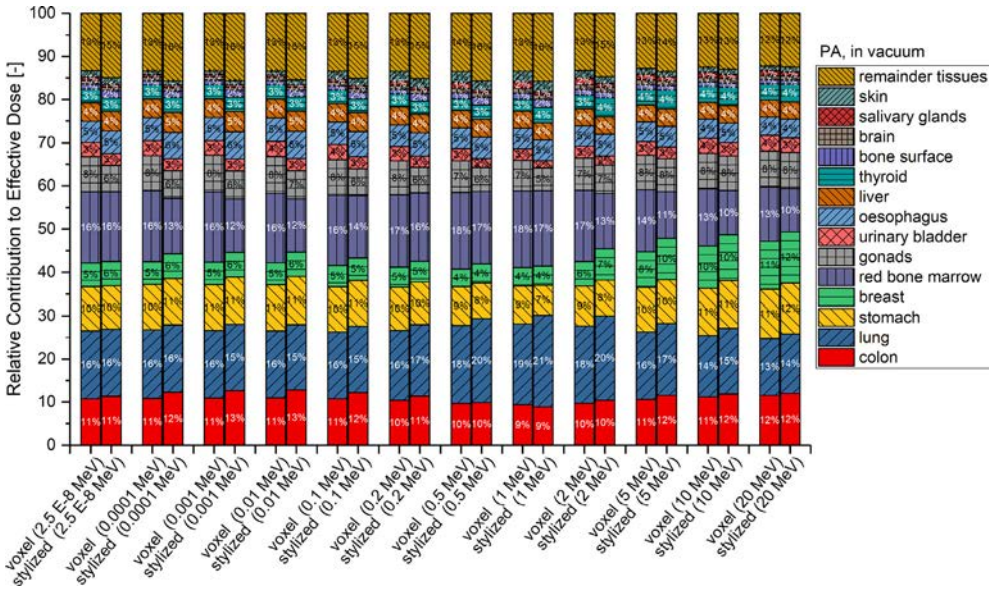

Fig. 6. Relative contribution of organs to the effective dose for the PA irradiation geometry: comparison of the stylized PIMAL phantom with the voxel phantom. (For a better interpretation of the number in the individual columns, the reader is kindly referred to the web version of this article.)

the results provided in (Bales et al., 2018) a much better agree ment with the dose conversion coefficients published by ICRP (ICRP, 2010) was obtained in the current study for neutron energy lager than 5 MeV.

- For the AP and ISO irradiation geometries, the effective dose val ues from the ICRP Publication 116 (ICRP, 2010) are well repre sented by the PIMAL phantom, with a relative deviation mainly within an interval $< \pm 5\%$. The largest deviation was observed at the neutron energy of 1 MeV, for which the ICRP dose conversion coefficient is 6.4% and 11.6% larger than the conversion coefficient obtained in this study for the AP and ISO irradiation geometry, respectively.
- For the PA irradiation geometry, the dose conversion coeffi cients obtained with PIMAL phantom in this study are in gen eral 5 10% larger than those published in the ICRP document, and the greatest difference occurs at 0.5 MeV, for which the stylized value obtained in this study is 14.2% larger than the ICRP value.
- For the LLAT and RLAT irradiation geometries, however, the dose conversion coefficients obtained in this study are in gen eral 15 20% lower than the ICRP values, and the greatest differ ence occurs at 1 MeV, for which the stylized values obtained in this study are 24.5% and 18.2% lower than the ICRP values for the LLAT and RLAT geometry, respectively.

In conclusion, the relatively large deviation as observed in the gender specific organ absorbed dose calculated with PIMAL and voxel phantom might be attributed to the different definition of the same organs in the two different phantoms, such as organ posi tion, shape, size (volume), density, material composition etc. How ever, for the effective dose, the PIMAL stylized phantom is comparable to its voxel counterpart. The stylized PIMAL phantom could serve as a reasonable surrogate for the relative complex ICRP/ICRU voxel phantom. This finding is in agreement with recent publications for external photon irradiation (Hiller and Dewji, 2017; Dewji et al., 2017). More importantly, the PIMAL phantom enables a convenient approach to define realistic body postures by moveable limbs, with which the influence of the body postures on the personal radiation exposure during working scenarios could be assessed.

3.2. Radiation exposure with realistic body postures in the emplacement drift

Fig. 8 compares the gender specific organ absorbed dose rate for the female and male PIMAL phantom in the emplacement drift at a distance of 1 m and 2 m to the POLLUX® lid surface for the real istic body postures sitting, walking and full bent as depicted in Fig. 3. The PIMAL phantom in the vertical upright posture serves as reference. The dimensionless organ absorbed dose rate ratios were calculated by dividing the different body postures' values by the vertical upright ones. The front body side was facing the lid surface of the POLLUX® type cask for all the investigated body postures.

For the sitting posture at 1 m distance, it is observed that the majority of the female and male organs have slightly larger absorbed dose values than their counterparts in the vertical upright posture, having ratios between 0.95 and 1.10. For the walk ing posture at the same distance, on the other hand, majority of the organs exhibit slightly lower absorbed dose than those in the vertical upright posture, having ratios between 0.95 and 1.00. Pos sible reasons for the difference between the two different body postures as observed above could be explained as follows:

- The walking posture investigated in the current study is quite similar to the vertical upright counterpart, except that the limbs are moved forward or backward, which might provide a certain but slight shielding effect for the internal organs.
- Compared to the cylindrical POLLUX® type cask disposed on the ground of the drift with an outer diameter of 1.56 m, the height of the PIMAL female phantom in vertical upright and sitting posture are 1.64 m and 1.34 m, respectively; the height of the PIMAL male phantom in vertical upright and sitting posture are 1.74 m and 1.45 m, respectively. Consequently, organs of the sitting phantom, especially those in the upper body part are slightly closer to the radiation source, i.e. the spent fuel

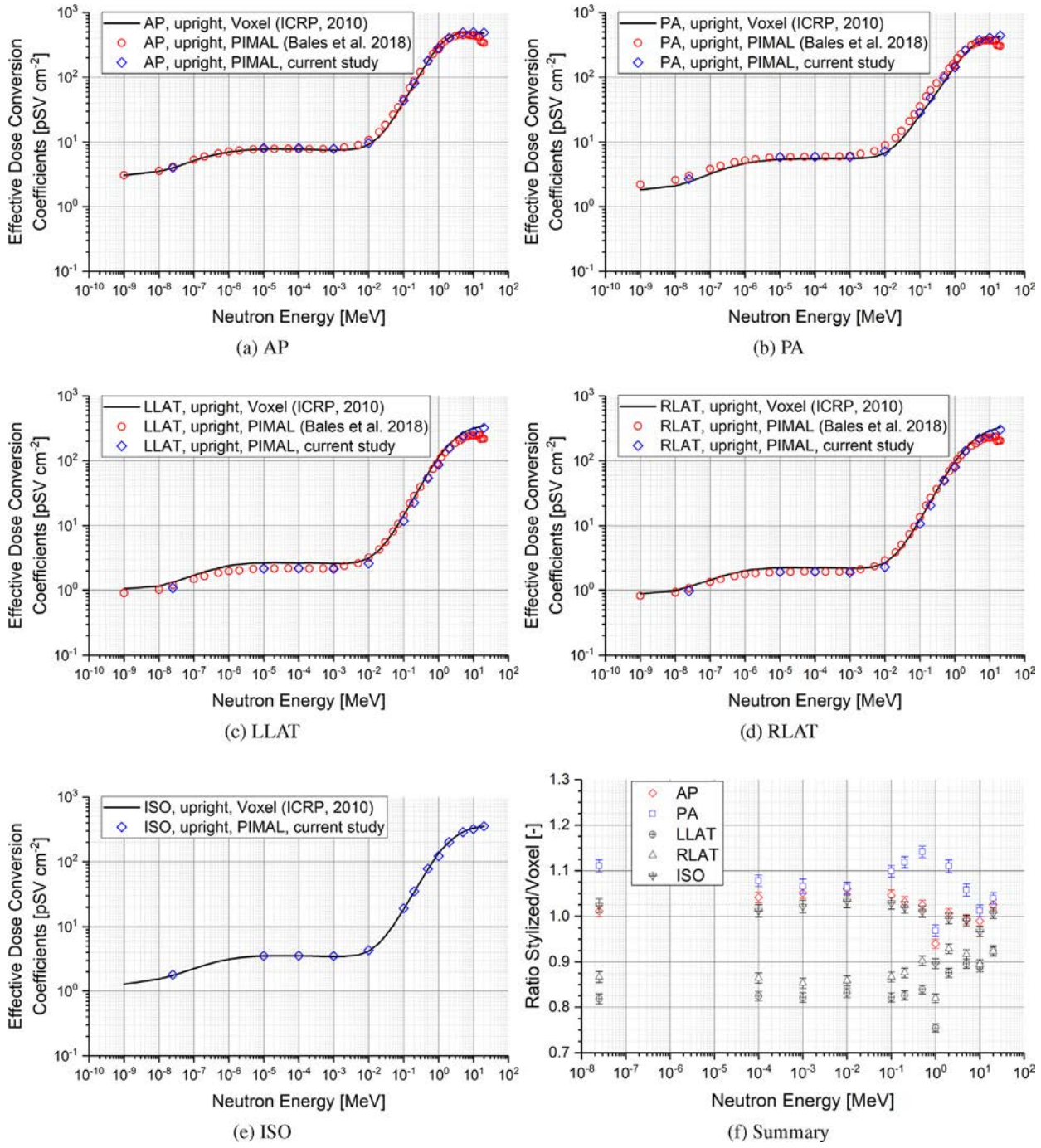

Fig. 7. Comparison of the effective dose coefficients obtained by the PIMAL phantom in vertical-upright posture with those given in (ICRP, 2010) for the standard irradiation geometry AP, PA, LLAT and RLAT.

loaded inside the cask. This might explain the slight higher organ absorbed dose for the PIMAL phantom in the sitting posture.

Nevertheless, it could be concluded that both sitting and walk ing postures show similar results compared to the vertical upright posture in terms of the organ absorbed dose rate. However, notable differences were observed for the full bent posture at 1 m distance:

- Since the distance of 1 m is measured between the center of pelvic area and the POLLUX® lid surface, with a full bent pos ture, the torso and especially the head of the phantom was bent over toward the lid surface of the POLLUX® type cask and their distance to the radiation source (SNF loaded inside the cask) is much less than 1 m. Consequently, organs such as the brain, the salivary glands, the thyroid receive a much higher exposure in the full bent posture compared to the case in the vertical upright posture. Furthermore, due to the

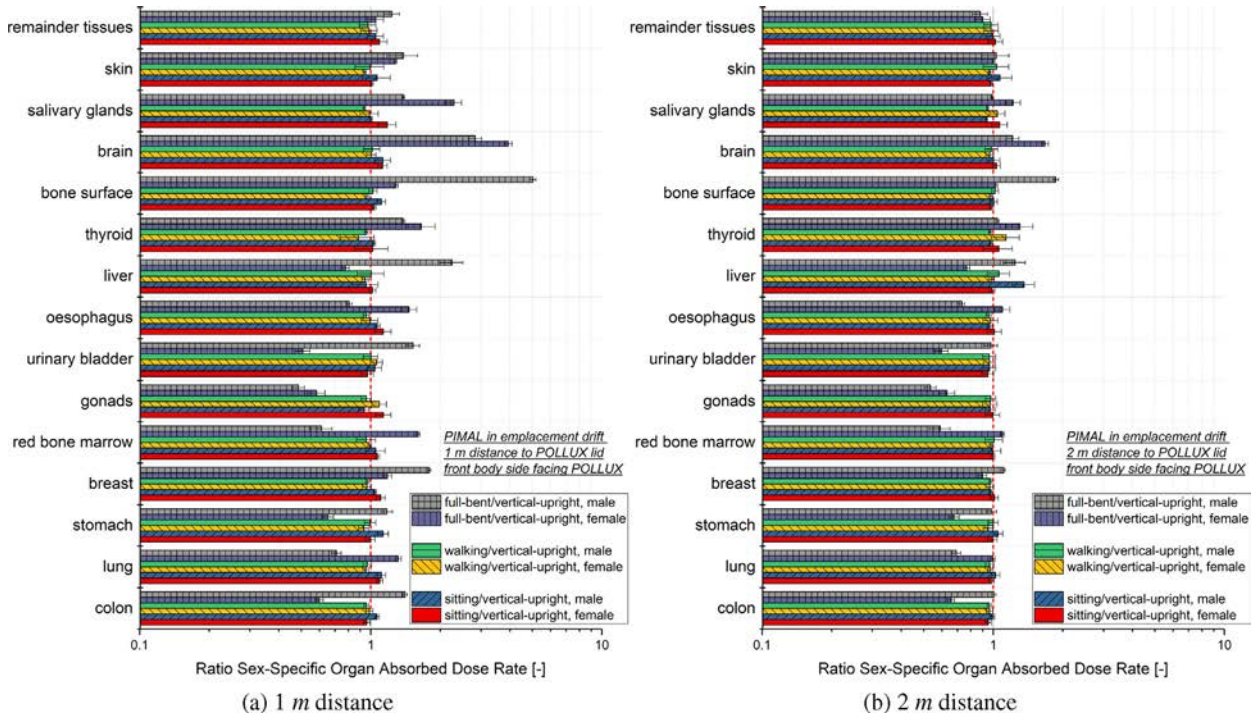

Fig. 8. Comparison of the gender-specific organ absorbed dose rate at 1 m and 2 m distance to the POLLUX® type cask for the body postures sitting, walking and full-bent. The vertical-upright posture was used as reference.

reduced distance of the upper body part to the POLLUX® type cask, organs such as the bone surface and the skin that are located close the surface of the body, as well as the breast that sticks out of the torso, experience also a larger organ absorbed dose compared to the case in the vertical upright posture.

- However, the bent torso enhances also the shielding effect for internal organs, especially those located in the abdomen and pelvic area. For instance, the gonads of the female and male phantom receive only 58.3% and 48.6% of the absorbed dose rate in the vertical upright position, respectively. However, among the critical organs with tissue weighting factor w_T 0.12, discrepancies were observed in colon, lung and stomach. For instance, the female colon and stomach receive an absorbed dose rate of less than 70% of that in the vertical upright posture, while the absorbed dose rate for the male colon and the male stomach in the full bent posture are 40.6% and 17.5% larger than their counterparts in the vertical upright posture. The reason for the discrepancies might be attributed to the combined effect of reduced distance and enhanced shielding.

Fig. 9 compares the gender averaged organ absorbed dose rate for the PIMAL phantom in the emplacement drift with realistic body postures representing a sitting, walking and full bent person. The gender averaged organ absorbed dose rate is required to assess the effective dose rate, with which the gender averaged organ equivalent dose rate is calculated by multiplication with the radiation weighing factor w_R of the neutrons. It is observed:

- At 1 m distance, especially the critical organs including colon, lung, stomach, breast, red bone marrow and the reminder tis sues of the PIMAL phantom for the sitting body posture receive a slightly higher (5 10%) organ absorbed dose than the PIMAL phantom in the vertical upright posture. However, as the dis tance to the POLLUX® type cask increases to 2 m, the difference between the realistic body postures and their vertical upright counterpart tends to decrease.
- Due to its closeness to the vertical upright posture, the walking body posture behave quite similar to the vertical upright pos ture, so that the gender averaged organ absorbed dose of the two postures agree well with each other with a difference in general less than 5% for the PIMAL phantom at both 1 m and 2 m distance to the POLLUX® type cask.
- As explained above, with a full bent torso two effects with con tradicting influence on the radiation exposure are to be expected: on the one hand, the distance of the organs in the head and the upper body part to the radiation source is reduced which might enhance the organ absorbed dose; on the other hand, the full bent torso increases the shielding for internal organs in the abdomen and pelvic area of the body. Conse quently, at 1 m distance, the first effect leads to a higher gender averaged organ absorbed dose especially for breast, bone surface and brain. However, with increasing distance to the POLLUX® type cask, the second effect of enhanced shielding plays a more significant role, so that the absorbed dose of the most critical organs including colon, lung, stomach and red bone marrow is only roughly 80% of that in the vertical upright posture. Furthermore, also due to the enhanced shield ing, the gonads in the full bent posture receives only an absorbed dose of about 60% of that in the vertical upright pos ture for both 1 m and 2 m distance.

Furthermore, Fig. 10 shows the relative contribution of the organs to the effective dose rate by taking into account the tissue weighting factor for the vertical upright, sitting, walking and full bent posture. For a given organ, the plot value in the figure is obtained as:

$$Relative\ Contribution \quad \frac{D_{T,gender\ \ averaged} \times w_T}{E} \tag{2}$$

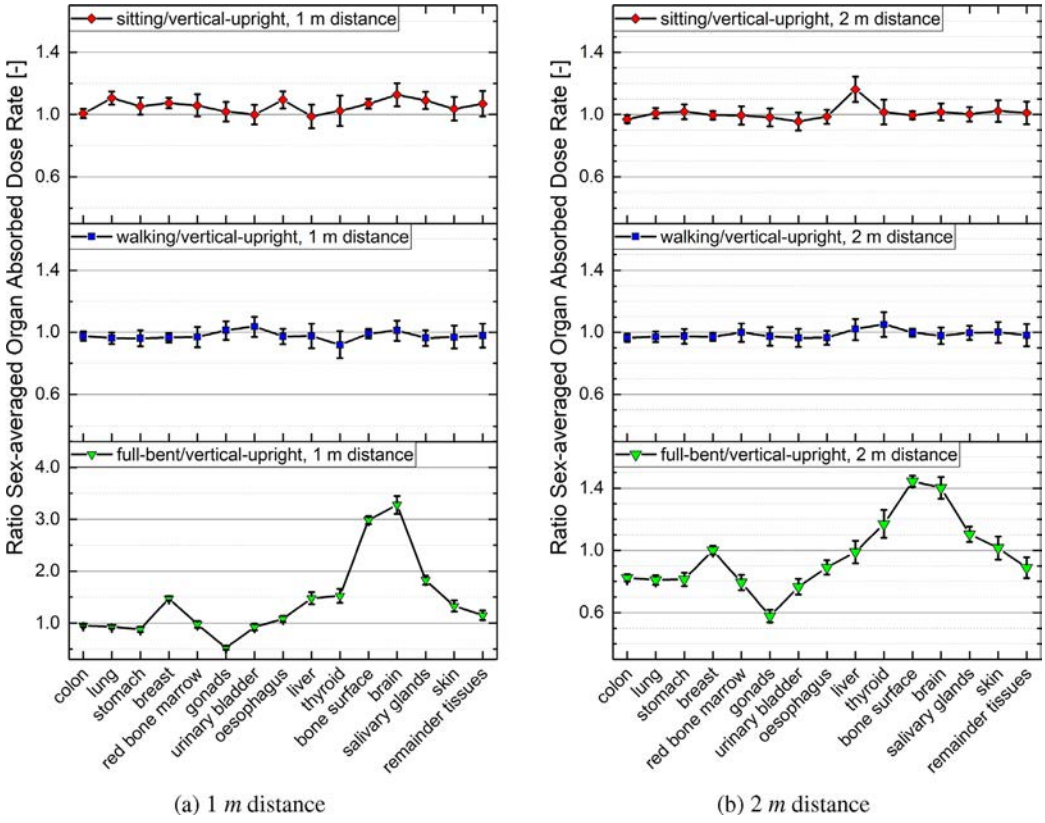

Fig. 9. Comparison of the gender-specific organ absorbed dose at 1 m and 2 m distance to the POLLUX® type cask for the realistic body postures sitting, walking and full-bent. The vertical-upright posture was used as comparison reference.

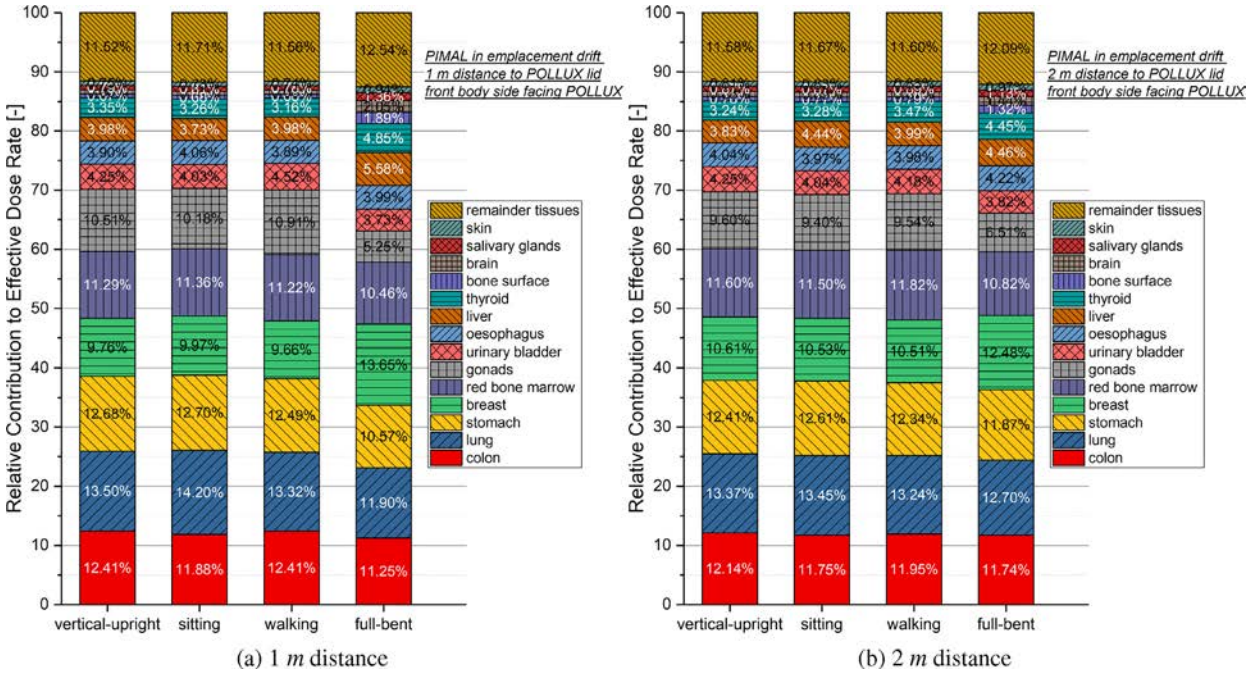

Fig. 10. Comparison of the relative contribution of the organs to the effective dose for the PIMAL phantom at 1 m and 2 km distance to the POLLUX® type cask for the realistic body postures vertical-upright, sitting, walking and full-bent.

where $D_{T,gender\ averaged}$ stands for the gender averaged organ absorbed dose. The radiation weighting factor w_R was not considered because the irradiation source was the same for all the investigated body postures at the same distance to the POLLUX® type cask. It is seen:

- Obviously, organs with relative larger tissue weighting factors w_T, including colon, lung, stomach, breast, red bone marrow, remainder tissues and gonads, contribute more significantly to the effective dose for all the investigated body postures.
- Furthermore, for the sitting and walking posture, the relative contribution of the different organs to the effective dose behave quite similar as for the vertical upright posture, which indicates that the influence of sitting and walking body posture could be neglected.
- However, some notable difference was observed for the full bent posture at 1 m distance, especially in breast with w_T 0.12 and in gonads with w_T 0.08. In terms of absorbed dose, organs such as brain, bone surface and thyroid exhibit also different behavior in the full bent posture, however, due to their relative lower tissue weighting factor, the difference is not that prominent in terms of organ contribution to effective dose. At 2 m distance, the organ contribution of the full bent posture is also similar to that of the vertical upright posture, except that of the gonads, for its gender averaged organ absorbed dose is only roughly 60% of that in the vertical upright posture.

Finally, Fig. 11 compares the effective dose of the three different body postures at 1 m and 2 m distance to the POLLUX® type cask. The effective dose of the PIMAL phantom in vertical upright posture was used as reference. Dimensionless effective dose rate ratios, obtained by dividing the different body posture values by the vertical upright ones, are plotted for the body postures sitting, walking and full bent. As expected, the effective dose rate of the PIMAL phantom in sitting and walking posture agree well with that in the vertical upright posture. The difference is in general less than 5% and tends to decrease with increasing distance of the phantom to the POLLUX® type cask. However, for the full bent posture, the effective dose at 2 m distance is only 85%) of that in the vertical upright posture, mainly due to enhanced shielding effect of the full bent torso for the internal organs as previously discussed.

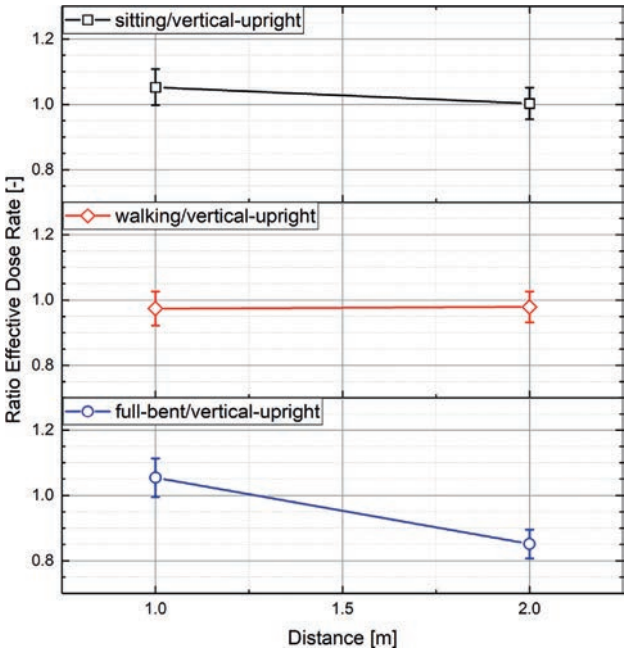

Fig. 11. Comparison of the effective dose rate at 1 m and 2 m distance to the POLLUX® type cask for the realistic body postures sitting, walking and full-bent. The vertical-upright posture was used as reference.

4. Conclusions and outlooks

In this study, a horizontal emplacement drift as part of a generic deep geological disposal facility for high level nuclear waste (HLW) in rock salt formation was modeled. In the rock salt drift, a nuclear waste package, simulated with a shielded cask loaded with spent nuclear fuel (SNF), was placed on the ground. A whole body stylized phantom with moveable limbs was applied to represent a reference worker inside the drift, whose individual body postures can be easily adapted with a graphical user interface. The stylized phantom in vertical upright posture was first assessed for calculation of neutron dose quantities in the standard external irradiation geometries including antero posterior (AP), postero anterior (PA), left and right lateral (LLAT, RLAT) and isotropic (ISO) configurations. The latest set of dose conversion coefficients provided by ICRP was used as comparison reference. Subsequently, radiation exposure for relevant body postures in the emplacement drift, including those representing a sitting person, a walking person and a person with full bent torso, was calculated with a general purpose Monte Carlo code. The phantom was placed at a distance of 1 m and 2 m to the lid surface of the disposed nuclear waste package. The main conclusions derived are summarized as follows:

(a) Despite differences in organ size, organ position, material composition etc. to its voxel counterpart, the PIMAL stylized phantom used in the current study is proven to be a suitable surrogate of the ICRP/ICRU reference adult voxel phantom for application in external neutron irradiation, with which the influence of realistic body postures, other than the vertical upright posture, on the personal radiation exposure during working scenarios could be assessed.

(b) At 1 m distance to the disposed waste package, the radiation exposure in terms of effective dose rate of a walking person in the emplacement drift is slightly lower ($< 5\%$) than that in the vertical upright posture, while the radiation exposure of a sitting person is up to 5% higher than that in the vertical upright posture. Furthermore, with increasing distance to the waste package, the influence of the sitting and walking body postures on the radiation exposure drops to a negligible level. This might be attributed to the fact that with increasing distance to the waste package, the radiation field in the emplacement drift tends to homogenize and to have a more isotropic character due to the increased amount of back scattering by the surrounding host rock layers.

(c) However, notable difference was observed for the full bent posture. Two effects with contrary influence on the radiation exposure are expected: on the one hand, the distance of the organs in the head and the upper body part to the radiation source is reduced which might enhance the organ absorbed dose; on the other hand, the full bent torso increases the shielding for internal organs in the abdomen and pelvic area of the body. At 1 m distance to the disposed waste package, the effective dose of the PIMAL phantom in the full bent posture is up to 5% higher than that in the vertical upright posture. However, with increasing distance to the waste package, the enhanced shielding effect of the full bent torso

for the internal organs plays a more significant role, so that at 2 m distance the effective dose of the full bent phantom is only 85% of that in the vertical upright posture.

(d) In conclusion, the sitting and walking posture behave quite similar to the vertical upright counterpart when assessing the radiation exposure in the emplacement drift. Consequently, the influence of the sitting and walking body postures on the personal exposure could be neglected. Furthermore, with increasing distance to the waste package, the enhanced shielding effect of the full bent torso for the internal organs leads to a lower radiation exposure compared to the vertical upright posture. Consequently, the vertical upright posture can also serve as a conservative estimate of the full bent posture.

To summarize, this paper contributes to the question whether the PIMAL phantom is suitable for such studies, when individual body postures are considered for a more realistic assessment of the personal radiation exposure. This is in particular necessary for planning and optimization of the working scenarios in retrieval of HLW. Remote access to handle the HLW waste packages during retrieval is often sought. A popular reasoning is that remote access to handle the waste packages would result in zero exposure. However, there are often cases for intervention when devices are not working properly or have to be readjusted or repaired in case of possible misfunctioning. Moreover, there are situations where working steps are not feasible with remotely controlled machines or such machines would be too costly or not robust enough for mining environment. In this case such simulations with the PIMAL phantom are valuable to be involved in the individual planning phase for devices/machines to foresee in advance shielding in case of intervention. With the methodology proposed in the current study, it could be shown that the PIMAL phantom is a planning requisite equivalent to the voxel counterpart including gender specific aspects, but with a much robust adjustment possibility to realistic body postures and much less computational effort, simultaneously. Hence, we encourage to its use.

However, possible limits should also be pointed out here. In the current state, it is unfortunately impossible to consider all interesting aspects concerning possible body postures during different phases of HLW management. Due to the lack of detailed (published) data, it is difficult to judge if different phase of management of HLW would require completely different body posture of the workers. At present, we assume that the basic postures can be considered similar all through the different phases. The present investigation could help to decide if different working scenarios, which could be realized in a different way including different postures, would yield a reduced exposure. This is in particular important when working close to the radiation source or for a longer time in the radiation field. This measure is also valid when shielding devices are employed, as the ALARA principle should be followed. The present results of this study provide an informative basis and could be generalized under the assumption that the exposure would scale direct proportional with the activity and effective shielding, depending on the different cask designs and related inventories. However, there is a lack of such information to justify this statement with a more detailed study, but it gives a future perspective to continue the investigation as far as the required details are available on a future proof basis.

Future prospects of this work are summarized as follows:

(a) First, it should be noted that in the current study the PIMAL phantom in realistic body posture was placed in the drift with the front body part facing the POLLUX® lid surface. Further investigations should be carried out, where the rear and lateral body part of the PIMAL phantom facing the POLLUX® lid surface, for further assessment of the conclusions derived in the current study. This could best be examined in future scenarios that are also to be implemented.

(b) In general, to fulfill the ALARA principle and to implement the radiation protection measures shielding distance time (length of stay) the evaluation of different possibilities in the planning phase can be realized. However, detailed (retrieval) plans are not yet available. Hence, in future when definite plans with details such as working tools, machines, cask types with inventories and sustainable storage/retrieval scenarios are available in the details needed for use oriented cases, it encourages for more in depth investigations.

CRediT authorship contribution statement

Bo Pang: Conceptualization, Methodology, Investigation, Writing original draft. **Frank Becker:** Conceptualization, Software, Investigation, Writing review & editing. **Volker Metz:** Conceptualization, Writing review & editing.

Declaration of Competing Interest

The authors declare that they have no known competing financial interests or personal relationships that could have appeared to influence the work reported in this paper.

Acknowledgement

The present study was supported partially by the Natural Science Foundation of Guangdong Province (Grant No. 2018A030313830).

Appendix

Table 1
Effective dose conversion coefficients obtained by the PIMAL stylized phantom for the standard irradiation geometries AP, PA, LLAT, RLAT and ISO. The table value "Ratio Stylized/Voxel" was calculated with the ICRP conversion coefficients (ICRP, 2010) as comparison reference.

Irradiation Geometry	Neutron Energy [MeV]	PIMAL Stylized [pGy cm ^{2}]	Ratio Stylized/Voxel [–]
AP	2.5×10^{-8}	4.05 ± 0.01	1.01 ± 0.01
AP	0.0001	8.11 ± 0.01	1.04 ± 0.01
AP	0.001	7.93 ± 0.01	1.05 ± 0.01
AP	0.01	9.66 ± 0.01	1.06 ± 0.01
AP	0.1	43.81 ± 0.05	1.05 ± 0.01
AP	0.2	81.27 ± 0.08	1.03 ± 0.01
AP	0.5	181.29 ± 0.16	1.02 ± 0.01
AP	1	282.83 ± 0.25	0.94 ± 0.01
AP	2	409.62 ± 0.34	1.01 ± 0.01
AP	5	490.70 ± 0.38	0.99 ± 0.01
AP	10	494.78 ± 0.37	0.99 ± 0.01
AP	20	489.17 ± 0.35	1.03 ± 0.01
PA	2.5×10^{-8}	2.71 ± 0.01	1.11 ± 0.01
PA	0.0001	6.01 ± 0.01	1.08 ± 0.01
PA	0.001	5.97 ± 0.03	1.07 ± 0.02
PA	0.01	7.24 ± 0.01	1.06 ± 0.01
PA	0.1	28.45 ± 0.04	1.10 ± 0.01
PA	0.2	48.20 ± 0.06	1.12 ± 0.01
PA	0.5	98.06 ± 0.10	1.14 ± 0.01
PA	1	143.33 ± 0.47	0.97 ± 0.01
PA	2	260.85 ± 0.76	1.11 ± 0.01
PA	5	374.46 ± 1.00	1.06 ± 0.01
PA	10	408.94 ± 1.01	1.01 ± 0.01
PA	20	439.72 ± 1.05	1.04 ± 0.01

Table 1 (*continued*)

Irradiation Geometry	Neutron Energy [MeV]	PIMAL Stylized [pGy cm ^{2}]	Ratio Stylized/Voxel [–]
LLAT	2.5×10^{-8}	1.08 ± 0.00	0.82 ± 0.01
LLAT	0.0001	2.18 ± 0.01	0.82 ± 0.01
LLAT	0.001	2.14 ± 0.01	0.82 ± 0.01
LLAT	0.01	2.60 ± 0.01	0.83 ± 0.01
LLAT	0.1	11.83 ± 0.03	0.82 ± 0.01
LLAT	0.2	22.47 ± 0.04	0.83 ± 0.01
LLAT	0.5	53.45 ± 0.09	0.84 ± 0.01
LLAT	1	86.77 ± 0.14	0.75 ± 0.01
LLAT	2	156.82 ± 0.22	0.88 ± 0.01
LLAT	5	241.01 ± 0.31	0.90 ± 0.01
LLAT	10	280.50 ± 0.32	0.89 ± 0.01
LLAT	20	321.13 ± 0.35	0.93 ± 0.01
RLAT	2.5×10^{-8}	0.97 ± 0.00	0.87 ± 0.01
RLAT	0.0001	1.93 ± 0.01	0.86 ± 0.01
RLAT	0.001	1.89 ± 0.01	0.85 ± 0.01
RLAT	0.01	2.29 ± 0.01	0.86 ± 0.01
RLAT	0.1	10.66 ± 0.02	0.87 ± 0.01
RLAT	0.2	20.50 ± 0.04	0.88 ± 0.01
RLAT	0.5	49.12 ± 0.08	0.90 ± 0.01
RLAT	1	79.81 ± 0.13	0.82 ± 0.01
RLAT	2	142.12 ± 0.20	0.93 ± 0.01
RLAT	5	219.90 ± 0.28	0.92 ± 0.01
RLAT	10	259.48 ± 0.31	0.89 ± 0.01
RLAT	20	302.76 ± 0.33	0.92 ± 0.01
ISO	2.5×10^{-8}	1.80 ± 0.01	1.02 ± 0.01
ISO	0.0001	3.58 ± 0.01	1.01 ± 0.01
ISO	0.001	3.53 ± 0.01	1.02 ± 0.01
ISO	0.01	4.33 ± 0.01	1.03 ± 0.01
ISO	0.1	19.14 ± 0.05	1.03 ± 0.01
ISO	0.2	35.06 ± 0.08	1.02 ± 0.01
ISO	0.5	77.88 ± 0.15	1.01 ± 0.01
ISO	1	122.76 ± 0.29	0.90 ± 0.01
ISO	2	202.01 ± 0.34	1.00 ± 0.01
ISO	5	287.18 ± 0.44	0.99 ± 0.01
ISO	10	320.88 ± 0.45	0.97 ± 0.01
ISO	20	354.34 ± 0.47	1.01 ± 0.01

References

Akkurt, H., Eckerman, K.F., Wagner, J.C., Sherbini, S., 2007. PIMAL: Computational phantom with moving arms and legs. Trans. Amer. Nucl. Soc. 96, 396.

Bales, K., Dewji, S., Sanchez, E., 2018. Comparison of neutron organ and effective dose coefficients for PIMAL stylized phantom in bent postures in standard irradiation geometries. Radiat. Environ. Biophys. 57, 375–393.

Dewji, S.A., Reed, K.L., Hiller, M., 2017. Comparison of organ doses for PIMAL stylized phantoms in upright and bent positions for standard irradiation geometries. Radiat. Environ. Biophys. 56, 277–291.

Herm, M., González-Robles, E., Müller, N., Dagan, R., Metz, V., 2018. Comparison of calculated and measured radionuclide inventory of a Zircaloy-4 cladding tube plenum section. MRS Adv. 3, 1031–1037.

Hiller, M., Dewji, S.A., 2017. Comparison of monoenergetic photon organ dose rate coefficients for the female stylized and voxel phantoms submerged in air. Radiat. Protect. Dosim. 175 (3), 336–343.

International Commission on Radiological Protection (ICRP), 1997. Conversion Coefficients for use in Radiological Protection against External Radiation. ICRP Publication 74..

International Commission on Radiological Protection (ICRP), 2007. The 2007 recommendations of the international commission on radiological protection. ICRP Publication 103. Annals of the ICRP 37..

International Commission on Radiological Protection (ICRP), 2009. Adult Reference Computational Phantoms. ICRP Publication 110. Annals of the ICRP 39(2)..

International Commission on Radiological Protection (ICRP), 2010. Conversion Coefficients for Radiological Protection Quantities for External Radiation Exposures. ICRP Publication 116, Annals of the ICRP 40(2-5)..

NEA, 2012. Reversibility of Decisions and Retrievability of Radioactive Waste. Nuclear Energy Agency, NEA No. 7085, pp. 29 (ISBN 978-92-64-99169-9)..

NEA, 2010. Reversibility and Retrievability in Planning for Geological Disposal of Radioactive Waste. Proceedings of the R&R International Conference and Dialogue, 14-17 December 2010, Reims, France, pp. 238 (ISBN 978-92-64-99185-9)..

Pang, B., Suárez, H.S., Becker, F., 2016. Individual dosimetry in disposal repository of heat-generating nuclear waste. Radiat. Prot. Dosim. 170 (1–4), 387–392.

Janberg, K., Spilker, H., 1998. Status of the development of final disposal casks and prospects in Germany. Nucl. Technol. 121, 136–147.

Pang, B., Becker, F., 2017. Albedo Neutron Dosimetry in a Deep Geological Disposal Repository for High-Level Nuclear Waste. Radiat. Prot. Dosim. 174 (3), 308–314.

Pang, B., Suárez, H.S., Becker, F., 2017a. Monte Carlo based study of radiation field in a deep geological repository for high-level nuclear waste with different host rock types. Nucl. Eng. Des. 325, 44–48.

Pang, B., Suárez, H.S., Becker, F., 2017b. Reference level of the occupational radiation exposure in a deep geological disposal facility for high-level nuclear waste: a Monte Carlo study. Ann. Nucl. Energy 110, 258–264.

Pelowicz, D.B. (Ed.), 2013. MCNP6 User's Manual. LA-CP13-00634, Rev. 0. Los Alamos National Security LLC., Los Alamos, NM.

Peiffer, F., McStocker, B., Gündler, D., Ewig, F., Thomauske, B., Havenith, A. and Kettler, J., 2011. Abfallspezifikation und Mengengerüst - Basis Ausstieg aus der Kernenergienutzung. Bericht zum Arbeitspaket 3: Vorläufige Sicherheitsanalyse für den Standort Gorleben. Gesellschaft für Anlagen- und Reaktorsicherheit. GRS-278, in German..

Röhlig, K.J., Häfner, D., Lux, K.-H., Hassel, T., Stahlmann, J., 2017. Einschluss oder Zugriff. Tiefenlagerung ohne oder mit Vorkehrungen zur Rückholbarkeit. Containment or Accessibility. Deep Disposal with or without Retrievability Measures. GAIA 26, 114–117.

Stahlmann, J., Mintzlaff, V. and Leon-Vargas, R., 2015. ENTRIA-Arbeitsbericht-03: Generische Tiefenlagermodelle mit Option zur Rückholung der radioaktiven Reststoffe: Geologische und Geotechnische Aspekte für die Auslegung. ISSN (Print): 2367–3532, ISSN (Online): 2367–3540, Technische Universität Braunschweig, Braunschweig, Germany, in German..

Spykman, G., 2018. Dry storage of spent nuclear fuel and high active waste in Germany - current situation and technical aspects on inventories integrity for a prolonged storage time. Nucl. Eng. Technol. 50, 313–317.

USNWTRB, 2018. Geologic Repositories: Performance Monitoring and Retrievability of Emplaced High-Level Radioactive Waste and Spent Nuclear Fuel. U.S. Nuclear Waste Technical Review Board report, pp 34..